Journal of Petroleum Science and Engineering 173 (2019) 492–500

Contents lists available at ScienceDirect

Journal of Petroleum Science and Engineering

journal homepage: www.elsevier.com/locate/petrol

Quantitative determination of the brittle–ductile transition characteristics of caprocks and its geological significance in the Kuqa depression, Tarim Basin, western China

Haixue Wang[a,b], Tong Wu[a,b,*], Xiaofei Fu[a,b,c], Bo Liu[a,b,c], Sheng Wang[a,b], Ru Jia[a,b,c], Chao Zhang[d]

[a] Laboratory of CNPC Fault Controlling Reservoir, Northeast Petroleum University, Daqing, China
[b] Science and Technology Innovation Team in Heilongjiang Province "Fault Deformation, Sealing and Fluid Migration", Daqing, Heilongjiang, China
[c] The State Key Laboratory Base of Unconventional Oil and Gas Accumulation and Exploitation, Earth Science College, Northeast Petroleum University, Daqing, China
[d] China Petroleum Tarim Oil Field Exploration and Development Institute, Kuerle, Xinjiang, China

ARTICLE INFO

Keywords:
Kuqa depression
Caprock
Brittle–ductile
Deformation mechanics
Vertical sealing

ABSTRACT

The Tarim Basin is one of the most hydrocarbon-bearing basins in China. It has two sets of gypsum and salt regional caprocks, which have various thicknesses and areal distributions. Such caprocks control large-scale hydrocarbon accumulation and the reservoirs formation in the basin. The estimation of the brittle–ductile transition characteristics of caprocks is one of the fundamental geological problems in petroleum exploration. To tackle this problem, a preliminary experimental method based on the mechanical characteristics of rocks is presented in this paper, which quantitatively forecasts the brittle–ductile transition characteristics of caprocks. The experimental study is based on triaxial tests on different gypsum and mudstones from caprocks of Jidike and Kumugeliemu Formations sheared at different confining stresses. It is shown that during burial, gypsums behave as normally consolidated materials and exhibit ductile responses to load increase. With the increase of depth, gypsum transforms from brittle stage to brittle–ductile or ductile stage. The confining pressure for brittle to brittle–ductile (semibrittle) transition of gypsum is about 18 MPa, and that of brittle–ductile to ductile transition is about 62 MPa. By analyzing the internal structure of fault zones from the caprocks in different brittle–ductile stages, it was observed that faults in brittle gypsum rock deform and form through-going faults, which are filled with soft fault gouge and often act as vertical migration pathways for hydrocarbon. Faults deformed in brittle–ductile caprocks form smears. A shale smear factor (SSF) of 3.5 is the critical value to discriminate between continuous and discontinuous gypsum smears, which can serve as a standard for determining the vertical sealing of the faults in brittle–ductile caprocks. It is generally difficult to cut through faults in ductile gypsum caprocks; this is significant to the sealing of the hydrocarbon vertical migration pathways.

1. Introduction

In oil and gas exploration, geologists have gradually realized that the caprock is one of the most important factors influencing large-scale hydrocarbon accumulation and reservoirs formation. The important properties mainly include the caprock lithology, cumulative thickness, caprock/strata ratio, individual layer thickness, and capillary pressure (Fu et al., 2008, 2015). The sealing capacity of caprocks is of great significance to natural gas preservation in China. Lv et al. (1996) recommended capillary pressure as the most direct and effective parameter for evaluating the seal capacity. However, relying on capillary pressure alone is not sufficient, as fractures (or faults) may alter caprock seal effectiveness (Ingram et al., 1997, 1999; Dewhurst et al., 1999; Nygard et al., 2006).

Rocks subjected to continual burial and never subjected to uplifting are called normal consolidation rocks. Normal consolidation rocks under continuous burial have brittle, brittle–ductile (semibrittle), and ductile characteristics (De Paola et al., 2009), which gradually change to brittle characteristics as the rocks are uplifted with decreased pressure. Moreover, fractures occur in brittle rocks with the increase of shear deformation, resulting in greater permeability and less sealing capacity (Jin et al., 2014). Faults deformed in brittle–ductile caprocks form smear structures. It is generally difficult to cut through the faults in ductile caprocks (Fu et al., 2015). In addition, brittle–ductile deformation is one of the most important factors that influences caprock integrity (Hangx et al., 2011; Carey and Frash, 2017). Brittle–ductile

* Corresponding author. Laboratory of CNPC Fault Controlling Reservoir, Northeast Petroleum University, Daqing, China.
E-mail addresses: wanghaixue116@163.com (H. Wang), 18845953084@163.com (T. Wu), fuxiaofei2008@sohu.com (X. Fu).

https://doi.org/10.1016/j.petrol.2018.10.042
Received 23 March 2018; Received in revised form 3 September 2018; Accepted 14 October 2018
Available online 16 October 2018
0920-4105/

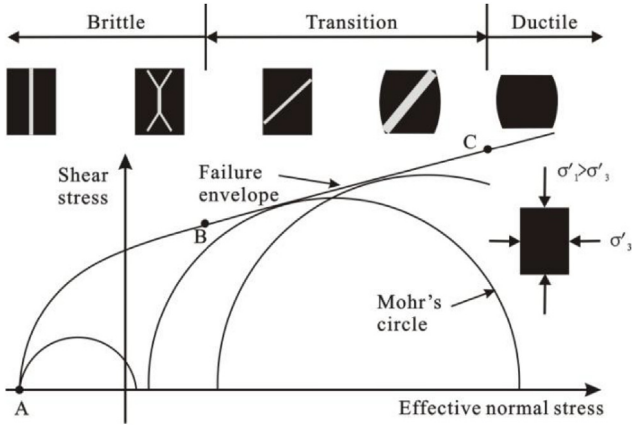

Fig. 1. Mohr diagram showing possible modes of failure, fracturing and brittle-ductile deformation (Nygard et al., 2006).

deformation varies with different lithologies and is dependent on the mechanical characteristics of the rocks (Fu et al., 2008; Paterson and Wong, 2005). Understanding this phenomenon is important for earth sciences and structural geology (Paterson and Wong, 2005).

Environmental conditions, such as pressure, temperature, and strain rate, are vital factors that affect brittle–ductile deformation. A rock may be brittle under some circumstances and ductile under others (Paterson and Wong, 2005). It has been confirmed with indoor triaxial experiments and field observations that brittle–ductile deformation significantly occurs in rock as the burial depth increases (Nygard et al., 2006; Brantut et al., 2011). Rocks undergo three deformation processes that correspond to the brittle, brittle–ductile transition, and ductile stages (Fig. 1). Rocks in the brittle stage are characterized by shear fractures and microfractures, which illustrates the strain softening characteristics. Local fractures develop, and the rocks undergo ductile deformation in the brittle–ductile transition stage (Fredrich et al., 1990; Evans et al., 1990). This stage is associated with strain hardening characteristics, and the stress drop, defined as the difference between failure stress and residual strength (Ismail and Murrell, 1990), decreases with increasing confining pressure. Rocks exhibit an acoustic emission response in the brittle and brittle–ductile transition stages (Yang, 2013). However, rocks have typical rheological characteristics in the ductile stage, and some of them exhibit fluidity; that is, they flow like syrup (Fossen, 2010), and no significant stress drop occurs (Ismail and Murrell, 1990). These rocks do not exhibit acoustic emission phenomena. The confining pressure has little effect in this stage; however, the rocks are sensitive to the temperature and strain rate. The main factors that influence brittle–ductile deformation are temperature and confining pressure (Byerlee, 1968; Kohlstedt et al., 1995). At a low confining pressure, the rocks are generally characterized by brittle deformation, but as the depth (confining pressure and temperature) increases, the rocks may transform into the brittle–ductile transition stage (even to the ductile stage) (Violay et al., 2012). Gypsum often acts as caprock, shielding oil and gas, and thus plays an important role in the oil industry. The fault deformation mechanism presents significant differences in caprocks in different brittle–ductile stages. However, the question of how to quantitatively determine the critical conditions of brittle–ductile transformation in caprocks with different lithologies has become a key point in research into the evaluation of the vertical sealing of faults. Based on the mechanical characteristics of rocks, Kohlstedt et al. (1995) first proposed a quantitative method for estimating the brittle–ductile stage of rock on a crustal scale. When Byerlee's friction rule (Byerlee, 1978) intersects the Mohr-Coulomb fracture envelope, rocks begin to transform from the brittle to the brittle–ductile transition region. The intersection of the Mohr-Coulomb fracture envelope with Goetze's criterion (Goetze, 1971) indicates the beginning of the ductile region. Ingram and Urai (1999) proposed a quantitative evaluation method for caprock brittleness that uses the clay brittleness index and rock density, which has a critical value. When the brittleness index is greater than 2, the likelihood of dilation behavior increases, and the risk of caprock leakage increases. Ingram and Urai (1999) and Nygard et al. (2004, 2006) presented the overconsolidation ratio, which can evaluate the critical condition of caprock leakage in the structural uplift process. When the overconsolidation ratio is greater than 2.5, the leakage risk of the caprock is higher.

The aims of this study are to take gypsum rich caprock of the Jidike Formation in the Kuqa depression as an example and combine the research results of Kohlstedt et al. (1995). A method for the quantitative description of the caprock brittle–ductile behavior is preliminarily established based on the mechanical characteristics of the rock. The experimental study is based on triaxial tests on gypsum- and mudstone-rich caprocks sheared at different effective confining stresses.

2. Geological settings

The Tarim Basin is a large multiple-superimposed basin that is composed of a marine Paleozoic intracratonic basin and a Meso-Cenozoic foreland basin with an ancient continental crustal substrate, which is a Proterozoic metamorphic rock series (He et al., 2009). Its northern boundary is the Tian Shan Mountains, and the southern borders are the Kunlun Mountains and the Altun Mountains. The basin trends nearly EW (Fig. 2). The Kuqa depression is located in the northern part of the Tarim Basin. Its strike is in NEE, and the basin is approximately 300 km in length in the EW direction, 30–80 km in the NS direction, and approximately 2.8×10^4 km^2 in area (Fu et al., 2006) (Fig. 2). Influenced by regional tectonic events, the Kuqa depression has undergone a complicated multiphase evolution: a foreland basin in the Late Permian to Triassic (260–205 Ma), an extensional depression basin in the Jurassic-Paleogene (205–23.3 Ma), and an intercontinental

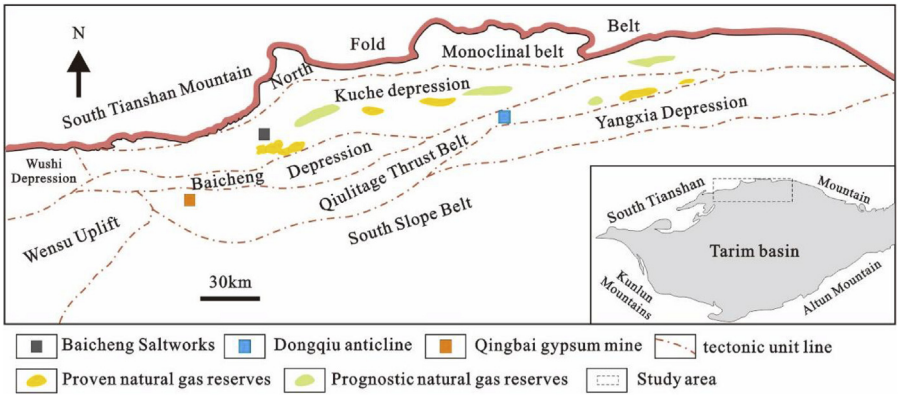

Fig. 2. Simplified structure distribution map of the Kuqa depression in the Tarim basin.

foreland basin in the Neogene-Quaternary (23.3–0 Ma) (Jia et al., 2003). The gypsum and salt caprocks in the Kumugeliemu Formation of the Paleocene-Eocene is one of the most important factors in large-scale natural gas accumulation in the Kuqa depression (Zhuo et al., 2013), which involves two main factors: (1) caprock quality (lithology, thickness, distribution, and capillary pressure) and (2) the brittle–ductile deformation of gypsum-rich caprocks and the vertical fault sealing ability. There is a steady distribution of gypsum and salt at the regional caprock in the Kuqa depression (Fu et al., 2008; Du et al., 2012). The capillary pressure of the caprock is generally greater than 15 MPa (Fu et al., 2008), and the sealing ability is very strong, which limits natural gas remigration and dissipation. However, there are still discoveries of oil and gas above the caprocks. Therefore, the basis of the vertical multi-layer distribution of natural gas is determined by the fault vertical sealing ability, which is controlled by the brittle–ductile characteristics of the rocks. In this study, based on rock mechanical characteristics tests and the internal structure of fault zone, the brittle–ductile process of gypsum rich caprock is systematically analyzed, and the vertical fault sealing ability is evaluated, in order to predict risk of oil and gas exploration.

3. Experiment procedure and method

3.1. Sample preparation and experimental environment

Cylindrical specimens with diameter of approximately 25 mm and height of approximately 50 mm were drilled. The sample height-to-diameter ratio was kept as close as possible to 2.5:1 to avoid problems of end effects as has been described by Paterson and Wong (2005). It is important that the specimen ends are parallel within a small tolerance less than 0.5 mm to ensure that the ends are flat and parallel and the errors in the height and diameter are less than 0.3 mm and 0.25 mm, respectively. The test specimens are in a natural state, and the test temperature is 25 °C with a humidity of 50%. Each sample was photographed prior to being placed into the experimental assembly.

3.2. Rock mechanics experiments procedure

The experiments were performed using a rock triaxial mechanical test system ($\sigma_1 > \sigma_2 = \sigma_3$) with high pressure, and was controlled by a TAW-2000 microcomputer, with a built-in pore fluid pressure system and a hydraulic oil confining pressure system. The maximum axial pressure of the triaxial test machine is 2000 kN. The temperature range varies from −50 °C to 200 °C. The load cell is located externally from the vessel and measures load on the upper piston of the sample assembly. The confining pressure was kept constant during deformation using a balanced piston arrangement. Axial force was applied using a servo-controlled electromechanical piston at a constant strain rate. All data, including confining pressure, strain, and load force, were measured and recorded in real-time using LabVIEW software.

Considering the variety of potential deformation mechanisms in the ductile field, one can expect a corresponding variety in the brittle–ductile transition characteristics when the physical mechanisms are considered. Thus, no single mechanistic view of the brittle–ductile transition can be valid under all conditions. First, we considered the nature of the transitions that can occur with increasing confining pressure at the corresponding temperature. We collected samples of white pure gypsum and mudstone from the Kuqa depression and carried out triaxial mechanical tests on 11 samples from each of the two groups shown in Table 1, but the pore fluid system was not used in these experiments. All the experiments were performed at controlled strain rates, and a constant strain rate of 0.03 mm/min was maintained throughout the experiment. The temperature in the triaxial loading experiments was calculated by the confining pressures on each experiment. The average geothermal gradient is 1.8–2.5 °C/100 m in the Kuqa depression (Wang et al., 2003), with an average annual surface temperature of 15 °C. Therefore, we could obtain the temperature in the different confining pressures (Table 1).

3.3. Quantitative determination method for the brittle–ductile transition characteristics of caprocks

Rock failure has two mechanisms: fracture and frictional sliding. Fracture is the only failure mechanism of intact rocks, and the fracture conditions are given by the Coulomb failure criterion, the Griffith criterion, the modified Griffith criterion, and the Mohr-Coulomb failure criterion (Griffith, 1920; Chen et al., 2009). Brittle shear fracture strength corresponds to the peak stress difference: it increases with increasing confining pressure. The Mohr-Coulomb failure criterion is considered an experimental criterion, and its envelope is generally a quadratic curve (Kohlstedt et al., 1995; Myrvang, 2001; De Paola et al., 2009), that is, the quadratic fitting curve of peak strength (shear rupture strength) in a stress-strain curve with different confining pressures (Petley, 1999). Sandstones with different porosities also have the same characteristics (Wong et al., 1997; 2004). If the rock is designed by a preexisting fault plane, the rock failure mechanism may be frictional sliding of the fault plane, which may also result in rupture through the fault surface. Research suggests that at a high confining pressure, friction may increase to such an extent that it requires as much stress to overcome friction as it does to cause faulting (Orowan, 1950; Wong and Baud, 2012). Hence, strength does not drop after faulting. The brittle–ductile transition may occur when friction along the fracture surface (Byerlee's rule) exceeds the shear strength (Mohr-Coulomb criterion) of the rock (Maurer, 1965) (Fig. 3). The type of failure depends upon whether the Mohr-Coulomb criterion (Fig. 3, purple line) or Byerlee's rule (Fig. 3, red line) is met by the rock (Chen et al., 2009).

3.3.1. When the Byerlee frictional strength exceeds the Mohr-Coulomb strength, it marks the end of brittle fracture

When the stress exceeded the yield point, brittle fracture occurred immediately in the rock, and the rock friction coefficient was almost constant under different confining pressures. The rock cohesion was approximately zero after fracturing. Because of the effects of shear stress, frictional sliding occurred in the rock, with the sliding friction coefficient and the coefficient of static friction being approximately equal. Based on a large number of rock friction sliding experiments, Byerlee (1968, 1978) suggested that to a useful approximation, the sliding friction of rock-on-rock is independent of rock type, characterized by a friction coefficient of 0.85 at small effective normal stresses and 0.6 at larger normal stresses. This relationship was supported by a compilation of experimental data. This is called the “Byerlee's rule.” Because the normal stress is generally lower than 200 MPa in the sedimentary basin, we applied the 0.85 friction coefficient from “Byerlee's rule":

$$\tau = 0.85\sigma_n \quad \sigma_n < 200\ MPa, \tag{1}$$

where τ is the shear stress (MPa), and σ_n is the normal stress (MPa).

The Byerlee's rule is independent of rock type and sliding surface (roughness), and it is universally applied to different natural friction sliding phenomena (Byerlee, 1978; Chen et al., 2009; Rutter and Glover, 2012).

Assuming that θ is the angle between the normal direction of the fault plane and the maximum principal stress in the rock, we can obtain the shear stress (τ) and normal stress (σ_n) as

$$\tau = \frac{\sigma_1 - \sigma_3}{2} \sin 2\theta, \tag{2}$$

$$\sigma_n = \frac{\sigma_1 + \sigma_3}{2} + \frac{\sigma_1 - \sigma_3}{2} \cos 2\theta, \tag{3}$$

where σ_1 and σ_3 are the maximum and minimum principal stresses (MPa), respectively.

With the limitation of $\theta \in (\frac{\pi}{4}, \frac{\pi}{2})$ and the shear fracture angle

Table 1
Mechanical parameters of the gypsum (Jidike formation) and mudstone (Kumugeliemu formation) caprock in the Kuqa depression.

Sample number	Lithology	Diameter (mm)	Height (mm)	*T* (°C)	Density (g/cm^3)	*Pc* (MPa)	Peak stress (MPa)	Residual stress (MPa)	Stress Drop (MPa)
9#	gypsum	25	50	25	2.65	0	17.7	4.9	12.8
13#	gypsum	25	50	25	2.65	5	34.5	28	6.5
7#	gypsum	25	50	25	2.65	20	73	62.9	9.1
5#	gypsum	25	50	25	2.65	40	77.6		
2#	gypsum	25	50	25	2.65	60			
1-14#	Salt mudstone	25	50	25	2.35	10	133	53	80
1-2#	Salt mudstone	25	50	35	2.36	20	143	84	59
1-4#	Salt mudstone	25	50	40	2.36	30	228	124	104
1-6#	Salt mudstone	25	50	50	2.35	40	250	143	107
1-8#	Salt mudstone	25	50	60	2.36	50	266	160	106
1-9#	Salt mudstone	25	50	65	2.34	55	284	176	108

$\theta = 45° + \tan^{-1}\mu/2$ (Byerlee, 1978; Chen et al., 2009; Rutter and Glover, 2012), we substitute θ into $\mu = \tan\varnothing$ ($\sigma_n < 200$ MPa) (where μ and ϕ are the coefficient of friction and the angle of internal friction of the rock, respectively) to obtain

$$\theta = 65.2° \ \sigma_n < 200\ MPa. \tag{4}$$

Substituting eqs. (2)–(4) into eq. (1) and using differential stress (σ_1–σ_3) and confining pressure (σ_3) coordinates, we can obtain the formula for the Byerlee's rule as eq. (5):

$$\sigma_1 - \sigma_3 \approx 3.7\sigma_3 \quad \sigma_3 < 100\ MPa, \tag{5}$$

where σ_1 and σ_3 are the maximum and minimum principal stresses (MPa), respectively.

Under low confining pressure (σ_3), the rocks exhibited pure brittle fracture, and the peak strength curve was a straight line with a slope that is similar to that of the sliding frictional curve (Byerlee's friction rule) after fracturing (Kohlstedt et al., 1995). With increasing confining pressure, some of the minerals in the rock exhibited ductile deformation, and both the internal friction angle and the sliding friction angle of the rock decreased. When the friction along the fracture surface was lower than the shear strength, the rocks were characterized by brittle fractures, which show strain softening, and the rocks met Byerlee's rule.

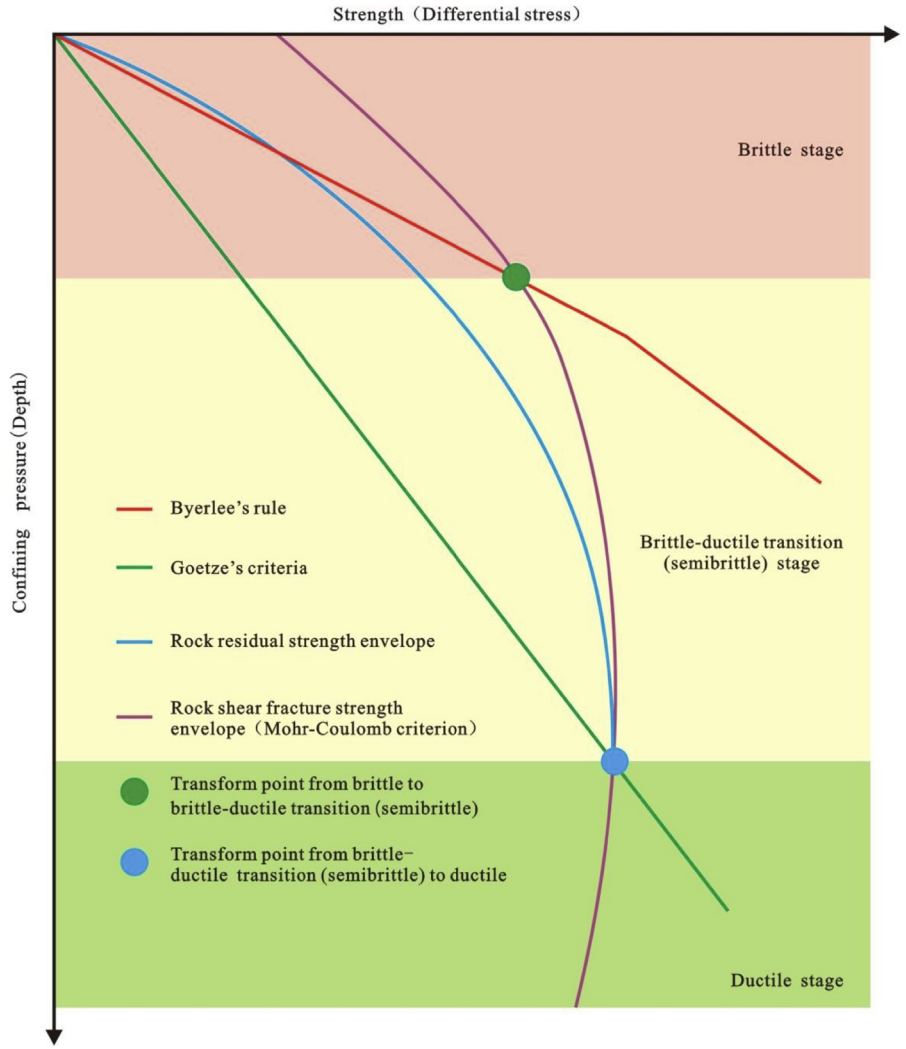

Fig. 3. The brittle ductile quantitative characterization method for the caprock (according to Kohlstedt et al., 1995; modified).

Moreover, when the Byerlee frictional strength exceeded the Mohr-Coulomb strength, which is the typical characteristic of strain hardening, it indicated that the rock met the Mohr-Coulomb criterion, and the rock will not slip along the existing fracture; this marks the end of brittle fracture, and the brittle–ductile (semibrittle) stage begins (Fig. 3).

3.3.2. Stress drop approaching zero is critical for ductile rock creep

Stress drop refers to the difference between the rock fracture peak strength and the residual strength (Petley, 1999). From a microscopic point of view, microfractures and the acoustic emission phenomena are generally associated with rocks in both the brittle and brittle–ductile transition stages. As shown in the stress-strain curves, the rocks exhibited appreciable stress drop. With increases in the confining pressure, the ductile components of rocks gradually increased, and the stress drop gradually decreased. When the confining pressure increased to a critical value, the stress drop tended toward zero. When the residual strength of the rock fracture envelope was consistent (coincident) with the Mohr-Coulomb fracture envelope, the ductile stage began (Fig. 3), and brittle fracture did not occur.

Goetze (1971) showed that when the stress drop is zero, most of the data indicate that the applied confining pressure (or effective confining pressure) is close to the fracture strength (σ_1–σ_3), which marks the transition from the brittle–ductile to the ductile flow stage (Fig. 3). This empirical criterion is Goetze's criterion (eq. (6)).

$$\sigma_1 - \sigma_3 \approx \sigma_3 \quad (6)$$

4. Experimental results

4.1. Rock material

The samples used in the experiment are gypsum and mudstone in the Jidike and Kumugeliemu Formations. They were recovered from field outcrops of Qingbai Gypsum Mine and Baicheng Saltworks of the Kuqa depression. The average densities of gypsum and mudstone are 2.65 and 2.35, respectively (Table 1). X-ray diffraction results are presented in Table 2. The data shows that the minerals of gypsum samples comprise gypsum (94.8%) and minor proportions of anhydrite (0.9%), quartz (2.1%), and siderite (2.2%) (Table 2). The minerals of mudstone samples comprise quartz (37.5%), plagioclase (21.8%), potassium feldspar (12.6%), calcite (8.4%), dolomite (6.8%), (salt 5.5%), and clay (7.4%) (Table 2).

4.2. The brittle–ductile deformation characteristics of caprocks

The experimental results show that the peak strength (shear rupture strength) and residual strength of both the white pure gypsum and the salt mudstone increased with increasing temperature and pressure (Table 1 and Fig. 4). Brittle deformation is more likely to occur when a material is stiff and has high shear strength. Brittle response and shear fracturing is more likely to occur at low effective stresses than at high stresses, as schematically shown in Fig. 1. The laboratory triaxial tests confirmed that the stress-strain curve suddenly changed when the rock fractured (Paterson and Wong, 2005), and that the cores developed shear fractures (Fig. 4a and b) and exhibited typical characteristics of strain softening and strain localization in the brittle stage.

At intermediate confining stresses, distinct shear fractures became more dominant without the formation of vertical fractures. The stress-strain curve gradually decreased (Yang, 2013) or gradually decreased after remaining constant for some time (Petley, 1999). The rock transformed to the brittle–ductile transition stage, local fractures and expansions were both present in the cores (Fig. 4a).

As the ductile field further developed with increase in the confining pressure, the macroscopic deformation became more pervasively distributed throughout the volume of the specimen, so that at confining pressures of several hundred megapascals, the deformation was essentially uniform, except for some restrictions caused by frictional end effects in the immediate vicinity of the ends. The stress-strain curve did not decrease after reaching its peak strength, and the stress drop tended toward zero. In addition, micro-fracture and emission phenomena disappeared (Evans et al., 1990; Yang, 2013), which is characteristic of expansion in the cores (Fig. 4a).

4.3. Definition of the critical conditions on the gypsum brittle–ductile transformation

The caprock in the Jidike and Kumugeliemu Formations of the Kuqa depression is dominated by gypsum and clay rock, and the gypsum is generally developed: the gypsum content of the entire formation is at least 10%. The quantitative characterization method was applied to the caprock brittle–ductile transformation stage, and we calculated that in the white gypsum, the critical confining pressure of the brittle to brittle–ductile transformation was 18 MPa. The critical confining pressure of the brittle–ductile to ductile transformation was 62 MPa (Fig. 5a). The critical confining pressure of the brittle to brittle–ductile transformation was 74 MPa in the mudstone. The critical confining pressure of the brittle–ductile to ductile transformation was 121 MPa (Fig. 5b). The experimental results show that the critical confining pressure of gypsum brittle–ductile transformation was lower than that of mudstone; that is, the mudstone exhibited brittle deformation with the same confining pressure, but gypsum might have transformed into the brittle–ductile deformation or even ductile deformation regime. Therefore, the critical depth of the brittle–ductile transformation for regional caprocks in the Jidike and Kumugeliemu groups is the critical condition for the gypsum brittle–ductile transformation.

5. Discussion

5.1. Factors influencing the brittle–ductile deformation of rocks

The focus of this study is to explore the brittle–ductile transition process of caprocks. Kohlstedt et al. (1995) first focused on the study of brittle–ductile variation at a crustal scale. Studies on the brittle–ductile deformation of caprocks at a basin scale mainly focused on the brittleness degree of the caprock (Ingram and Urai, 1999; Nygard et al., 2004, 2006). The factors affecting the brittle–ductile behavior of caprocks mainly include internal causes (e.g., lithology, mineral composition, and properties) and external causes (e.g., temperature, pressure, fluid pressure, oiliness, water content, and tectonic uplifting). The

Table 2
Mineralogical characteristics of gypsum and mudstone samples in the Kuqa depression.

Sample No.	Sample Source	Whole rock mineralogy (wt%)									
		Q	P	Cal	Dol	Sid	PF	G	An	S	TC
QBGM 1	Gypsum	2.1				2.2		94.8	0.9		
BCS 3	Mudstone	37.5	21.8	8.4	6.8		12.6			5.5	7.4

Q: quartz; PF: Potassium feldspar; P: plagioclase; Cal: calcite; Dol: dolomite; Sid: Siderite; G: Gypsum; An: Anhydrite; S: Salt; TC: Total Clay, QBGM: Qingbai gypsum mine. BCS: Baicheng Saltworks.

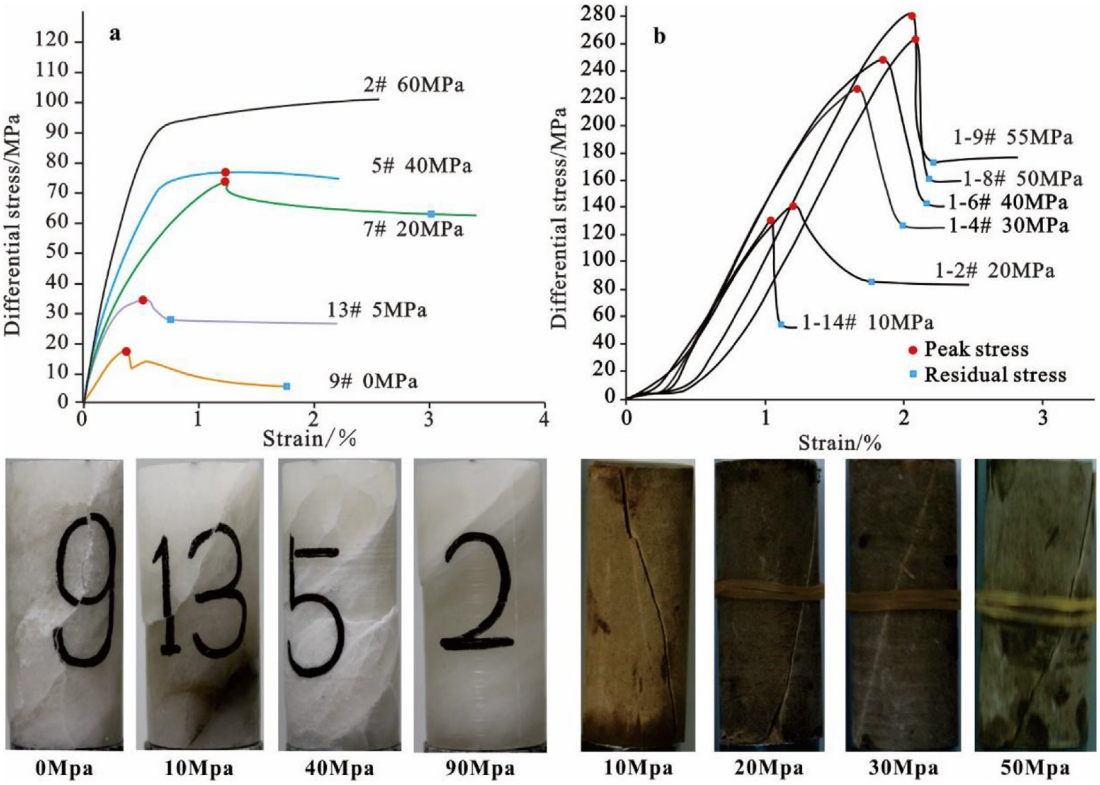

Fig. 4. The stress-strain curves and core photos after fracturing at various confining pressures. (a) White gypsum in the Qingbai Gypsum Mine. (b) Salt-mudstone in the Baicheng Saltworks.

mechanical characteristics are the key properties of rocks. This study is based on the brittle–ductile quantitative characterization method of Kohlstedt et al. (1995) and drew on the findings of previous research into brittle–ductile deformation in the sandstone deformation zone. We establish a quantitative description method of the brittle–ductile transformation phase, and the confining pressure and temperature are considered. The brittle–ductile zone of rocks is divided into three regions: the brittle region (I), the brittle–ductile transition region (II), and the ductile region (III). The stress-strain curve changed suddenly in the brittle region, and shear fractures developed in the cores. The stress-strain curve gradually decreased (Yang, 2013) or gradually decreased after remaining constant in the brittle–ductile transition region, which resulted in the development of a typical shale smear structure. In the ductile stage, the stress-strain curve did not decrease after reaching its peak strength, and it even continued to increase with increasing depth (Fig. 6). Triaxial laboratory tests of oil-bearing clay samples confirmed

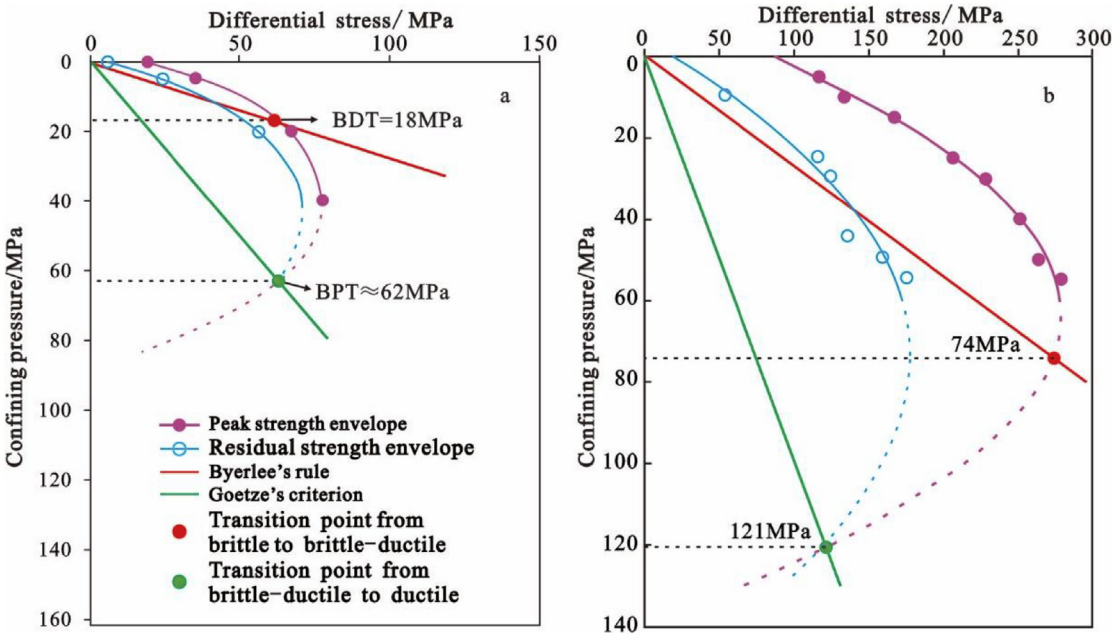

Fig. 5. The critical confining pressure of the brittle-ductile transition in caprocks of different lithologies. (a) White gypsum in the Qingbai Gypsum Mine. (b) Salt mudstone in the Baicheng Saltworks. The dotted line represents the forecast trend.

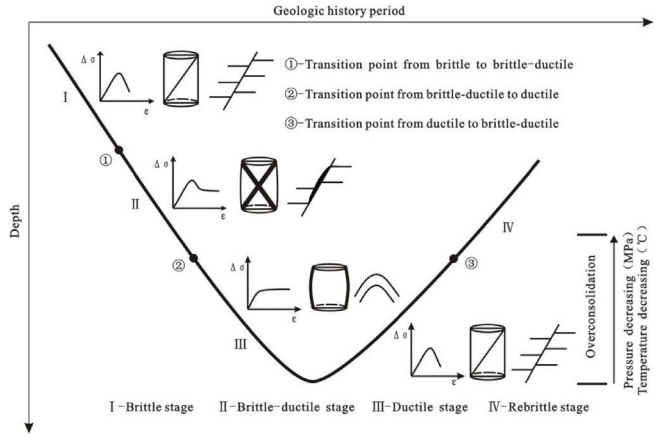

Fig. 6. The relationship between burial history of gypsum and brittle-ductile transformation.

(Nygard et al., 2006) that oiliness decreased the critical confining pressure of the clay brittle–ductile transformation. However, the influence of fluid pressure, oiliness, water content, diagenesis, strain rate, and tectonic uplift on the brittle–ductile deformation of caprock was not considered in this study.

5.2. Research relating structural uplift to the brittle–ductile transformation of rocks

Basins generally experience tectonic uplifts that result in the confining pressure reduction. As the confining pressure decreases, the rock may change from ductile deformation to brittle deformation, which is the rebrittle phase (IV) (Fig. 6). Currently, there are mainly two methods for determining the critical condition of ductile–brittle transformation of clay. One is the overconsolidation ratio (Nygard et al., 2004, 2006), which evaluates the brittleness degree of caprock under tectonic uplift conditions. Its critical value is 2.5. When the overconsolidation ratio is greater than 2.5, the vertical leakage probability of clay caprock is very high. The other is a preliminary idea based on the triaxial laboratory tests. We loaded a certain confining pressure, and although the axial pressure gradually increased, the peak value of the stress-strain curve did not reduce, demonstrating that the rock has reached the ductile stage. In addition, with the axial stress kept constant, we gradually decreased the confining pressure until the rock began to exhibit shear fracturing. The value of this confining pressure may be the critical value for the transformation from ductile to brittle stage.

5.3. The internal structure of the fault zone and vertical sealing

Caprock in the brittle stage was characterized by brittle fracturing because of the macroscopic deformation characteristics of the field, e.g., the brittle faults in the Baicheng Saltworks of the Kuqa depression, where the salt-layer developed brittle fractures, and fault gouge filled the fault zone; the fault gouge included a substantial amount of salt. If we remove its hard surface, the internal fault gouge would be similar to a “soft surface.” The thickness of the fault zone was approximately 25 cm (Fig. 7). In the brittle–ductile transition stage, the caprock was typically characterized by clay smear. The gypsum was dragged into the fault zone in the Dongqiu anticline where brittle–ductile transition deformation occurred, which caused the formation of shear clay smear (Fig. 8a and b). The gypsum and salt exhibited flow characteristics in the ductile stage. They flowed and extruded along the fault and occurred at the highest point of the fault, which expresses typical ductile deformation. For example, the sandstones of the Jidike Formation and the salt rock of the Kumugeliemu Formation were exposed on the surface in the Xiqiu structural zone (Fu et al., 2015).

The Kuqa depression extensively developed gypsum in the Paleogene Kumugeliemu Formation and the Neogene Jidike Formation, which constituted the regional caprocks of the basin. The deformation mechanism of both faults in the caprock and fault zone structure directly determined the amount of oil and gas accumulation and dissipation. With increase in the burial depth, the brittle–ductile transformation characteristics of the gypsum, salt, and mudstone increased (Nygard et al., 2006). The mechanical characteristics of the gypsum and field observations were used to classify the internal structure of the fault zone into three deformation regions. Through-going faults usually formed in brittle salt rock, gypsum rock, and clay rock, and the fault zone was usually filled with soft fault gouge, e.g., the faults in the North limb of the Dongqiu anticline and the Baicheng salt field (Fig. 7). These faults formed vertical hydrocarbon migration pathways in the active stage. Shear shale smear is interpreted to be responsible for the attenuation of clay smears observed with increasing distance from source beds (Vrolijk et al., 2016) and formed in the brittle–ductile regime. The competent units (mudstone layer) were deformed in a brittle mode, given that the tensile strength of rocks was lower than their shear strength. The gypsum unit simply reacted to this offset in a ductile manner. The gypsum formed a typical smear structure in the brittle–ductile transition region (Fig. 8a). Currently, shale smear factor (SSF), the ratio of throw to thickness, is used to evaluate the continuity of shale smear (Yielding et al., 1997; Takahashi, 2003; Faerseth, 2006; Fu et al., 2012; Vrolijk et al., 2016). Based on a detailed investigation (throw and thickness of gypsum layer) of continuous and discontinuous gypsum smear faults in the south limb of the Dongqiu anticline, the critical SSF of the continuous gypsum-clay smear may be 3.5–4.0 (Fig. 8). If the clay smear maintains continuity, the fault will be vertically sealed. Based on numerical simulations and field geological surveys, Welsh et al. (2009) determined that the thrust fault clay smear is controlled by fault throw, clay thickness, geometry, size, and propagation rate, and the maximum critical SSF value for continuous shale smear is 4.6. The gypsum exhibited flow characteristics in the ductile region, along with fault thrust sliding. Gypsum and salt flowed along the fault surface and extruded at the thrust belt front, e.g., the exposed extensive gypsum and salt in the Kumugeliemu Formation of the Xiqiu anticline thrust sheet front, Kuqa depression (Fu et al., 2015).

6. Conclusion

This study attempts to build a preliminary experimental method that quantitatively predicts the brittle–ductile transition characteristics of caprocks, based on the mechanical characteristics of rocks and field observations. The following conclusions can be drawn:

- Based on the Mohr-Coulomb criterion, Byerlee's rule, and residual strength (or Goetze's criterion), combined with the stress-strain curve and shear failure characteristics, we utilized a preliminary experimental method to quantitatively predict the brittle–ductile transition characteristics of caprock. The brittle to brittle–ductile transition and brittle–ductile to ductile transition occurs at critical confining pressures (*Pc*) of about 18 MPa and 62 MPa, respectively, in the pure white gypsum, and about 74 MPa and 121 MPa, respectively, in the mudstone.
- Fault deformation in brittle gypsum caprocks results in through-going faults filled with gouge. It also results in a smear structure, and an SSF of 3.5 is the threshold between continuous and discontinuous gypsum smears, which can be taken as the criterion for determining the vertical sealing ability of faults in brittle–ductile gypsum caprocks. Generally, faults cannot cut through ductile gypsum caprocks; therefore, the caprocks can act as natural gas seals.
- Therefore, the brittle–ductile transition characteristics of caprocks and the internal structure of the fault zone are the key determinants

Fig. 7. The development characteristics of a fault in the brittle salt caprock of the Baicheng Saltworks (for its position, see Fig. 2). (a) The macroscopic characteristics of the brittle fault zone. (b) The fault zone and its thickness.

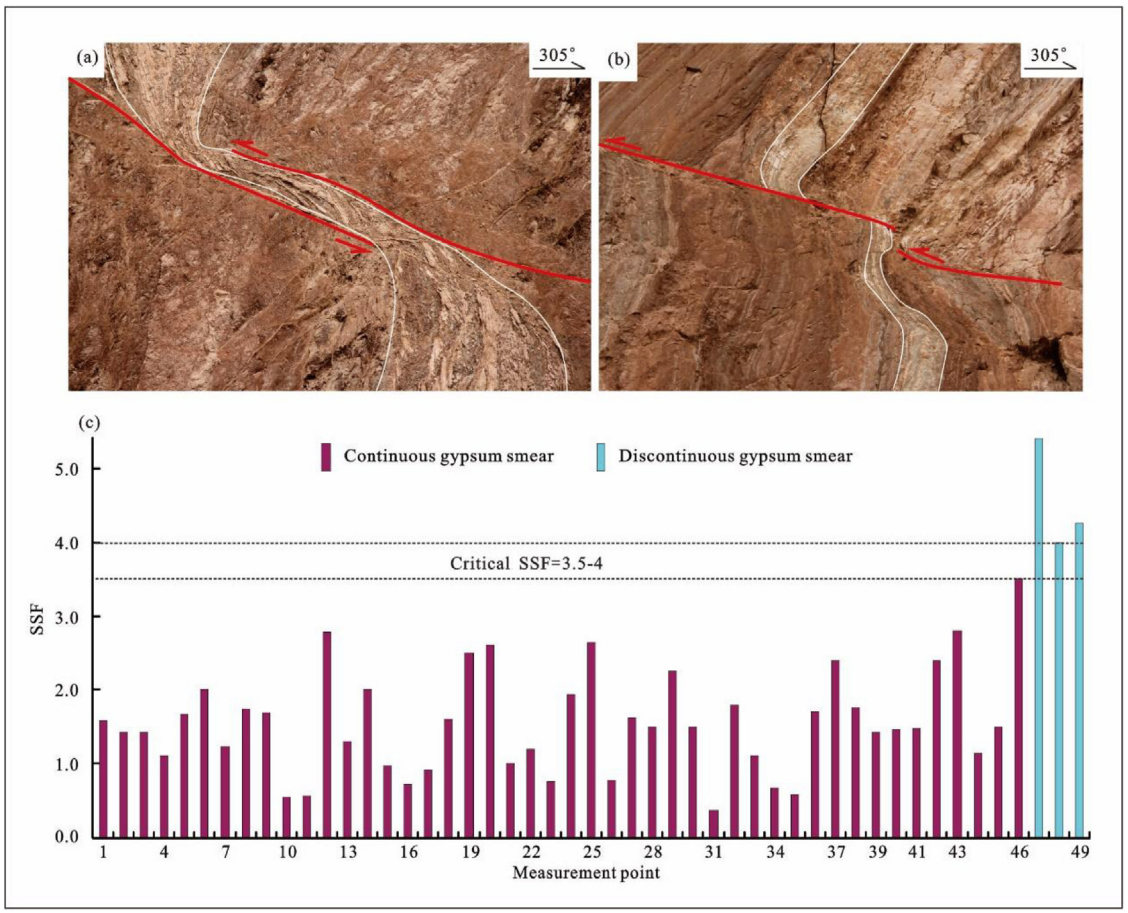

Fig. 8. The fault zone structure of brittle-ductile gypsum and critical SSF in the Kumugeliemu group of the Kuqa depression. The development characteristics of continuous smear (a) and Discontinuous smear (b) in the thrust fault of the South limb of the Dongqiu anticline (for its position, see Fig. 2). The critical SSF of gypsum smear at the measuring point (c).

of fault vertical sealing evaluation, which control the vertical distribution of gas in the Tarim Basin.

Acknowledgments

This study was financially supported by the Provincial Natural Science Foundation of Heilongjiang (No. QC2018041), the National Natural Science Foundation of China (No. 41602129, U1562214, 41472125), and National Basic Research Program of China (No. 2016ZX05003-002). The authors thank the China Petroleum Science and Technology Research Institute and the Tarim Oilfield.

References

Brantut, N., Schubnel, A., Guéguen, Y., 2011. Damage and rupture dynamics at the brittle-ductile transition: the case of gypsum. J. Geophys. Res. Solid Earth 116, 1–19 B01404.
Byerlee, J.D., 1968. Brittle-ductile transition in rocks. J. Geophys. Res. 73, 4741–4750.
Byerlee, J.D., 1978. Friction of rocks. Pure Appl. Geophys. 116 (4–5), 615–626.
Carey, J.W., Frash, L.P., 2017. Brittle-ductile behavior and caprock integrity. Energy Procedia 114, 3132–3139.
Chen, Y., Huang, T.F., Liu, E.T., 2009. Rock Physics. University of Science & Technology China press, pp. 112–192.
Dewhurst, D.N., Yang, Y., Aplin, A.C., 1999. Permeability and fluid flow in natural mudstones. In: Geological Society, vol. 158. Special Publications, London, pp. 23–43.
De Paola, N., Faulkner, D.R., Collettini, C., 2009. Brittle versus ductile deformation as the main control on the transport properties of low-porosity anhydrite rocks. J. Geophys. Res. Solid Earth 114 (B06211), 1–17.
Du, J.H., Wang, Z.M., Hu, S.Y., Wang, Q.H., Xie, H.W., 2012. Formation and geological characteristics of deep giant gas provinces in the Kuqa foreland thrust belt, Tarim basin, NW China. Petrol. Explor. Dev. 39 (4), 385–393.
Evans, B., Frederich, J.T., Wong, T.F., 1990. The brittle-ductile transition in rocks: recent experimental and theoretical progress. In: In: Duba, A.G., Durham, W.B., Handin, J.W., Wang, H.F. (Eds.), The Brittle-ductile Transition in Rocks. The Heard Volume: American Geophysical Union, vol. 56. Geophys Monograph, Washington, D.C, pp. 1–20.
Faerseth, R.B., 2006. Shale smear along large faults: continuity of smear and the fault seal capacity. J. Geol. Soc. 163, 741–751.
Fossen, H., 2010. Structural Geology. Cambridge University Press, New York, pp. 119–185.
Fredrich, J.T., Evans, B., Wong, T.F., 1990. Effect of grain size on brittle and semibrittle strength: implications for micromechanical modeling of failure in compression. J. Geophys. Res. 95, 10907–10920.
Fu, X.F., Guo, X., Zhu, L.X., Lv, Y.F., 2012. Formation and evolution of clay smear and hydrocarbon migration and sealing. JJ. China Univ. Min. Technol. 41 (1), 52–63.
Fu, X.F., Jia, R., Wang, H.X., Wu, T., Meng, L.D., Sun, Y.H., 2015. Quantitative evaluation on the fault-caprock sealing: examples from Dabei-Kelasu structural belt in Kuqa Depression, Tarim Basin. Petrol. Explor. Dev. 42 (3), 1–10.
Fu, X.F., Liu, X.B., Song, Y., Liu, S.B., 2008. Caprock quality and hydrocarbon accumulation in the basins of foreland thrust belts, Central and Western China. Geol. Rev. 54 (1), 82–93.
Fu, X.F., Song, Y., Lv, Y.F., Sun, Y.H., 2006. Rock mechanic characteristics of gysum cover and conservation function to gas in the Kuqa depression, the Tarim basin. Pet. Geol. Exp. 28 (1), 25–29.
Goetze, C., 1971. High temperature rhelogy of westerly granite. J. Geophys. Res. 76 (5), 1223–1230.
Griffith, A.A., 1920. The phenomena of rupture and flow in solids. Phil. Trans. Roy. Soc. Lond. A221, 163–198.
Hangx, S.J.T., Spiers, C.J., Peach, C.J., 2011. The mechanical behavior of anhydrite and the effect of deformation on permeability development–implications for caprock integrity during geological storage of co_2. Energy Procedia 4 (1), 5358–5363.
He, D.F., Zhou, X.Y., Yang, H.J., Lei, G.L., Ma, Y.J., 2009. Geological structure and its controls on giant oil and gas fields in Kuqa depression: a clue from new shot seismic data. Geotect. Metallogenia 33 (1), 19–32.
Ingram, G.M., Urai, J.L., 1999. Top-seal leakage through faults and fractures: the role of mudrcok properties. Geol. Soc. Lond. 158, 125–135.
Ingram, G.M., Urai, J.L., Naylor, M.A., 1997. Sealing processes and top seal assessment. In: Norwegian Petroleum Society, vol. 7. Special Publications, pp. 165–174.
Ismail, I.A.H., Murrell, S.A.F., 1990. The effect of confining pressure on stress-drop in compressive rock fracture. Tectonophysics 175 (1), 237–248.
Jia, C.Z., Wei, G.Q., Li, B.L., Xiao, A.C., Ran, Q.G., 2003. Tectonic evolution of two-epoch foreland basins and its control for natural gas accumulation in China's mid-western areas. Acta Pet. Sin. 24 (2), 13–17.
Jin, Z., Yuan, Y., Sun, D., Liu, Q., Li, S., 2014. Models for dynamic evaluation of mudstone/shale cap rocks and their applications in the lower paleozoic sequences, sichuan basin, sw china. Mar. Petrol. Geol. 49, 121–128.
Kohlstedt, D.L., Evans, B., Mackwell, S.J., 1995. Strength of the lithosphere:Constraints imposed by laboratory experiments. J. Geophys. Res. 100 (B9), 17587–17602.
Lv, Y.F., Fu, G., Gao, D.L., 1996. The Reservoir Cap Rock Research. Petroleum Industry Press, Beijing, pp. 30.
Maurer, W.C., 1965. Shear failure of rock under compression. Soc. Petrol. Eng. J. 5, 167–175.
Myrvang, A., 2001. Rock Mechanics. Norway University of Technology (NTNU), Trondheim Trondheim (in Norwegian).
Nygard, R., Gutierrez, M., Bratli, R.K., Høeg, K., 2006. Brittle–ductile transition, shear failure and leakage in shales and mudrocks. Mar. Petrol. Geol. 23, 201–212.
Nygard, R., Gutierrez, M., Gautam, R., Høeg, K., 2004. Compaction behavior of argillaceous sediments as function of diagenesis. Mar. Petrol. Geol. 21, 349–362.
Orowan, E., 1950. Mechanism of seismic faulting, rock deformation. Geol. $oc. Am. Mem. 79, 323–345.
Paterson, M.S., Wong, T.F., 2005. Experimental Rock Deformation-the Brittle Field. Springer, New York, pp. 1–347.
Petley, D.N., 1999. Failure envelops of mudrocks at high confining pressures. Geol. Soc., Lond., Special Publications 158 (1), 61–71.
Rutter, E.H., Glover, C.T., 2012. The deformation of porous sandstones; are Byerlee friction and the critical state line equivalent? J. Struct. Geol. 44, 129–140.
Takahashi, M., 2003. Permeability change during experimental fault smearing. J. Geophys. Res. 108 (B5), 1–15.
Violay, M., Gibert, B., Mainprice, D., Evans, B., Dautria, J., Azais, P., et al., 2012. An experimental study of the brittle-ductile transition of basalt at oceanic crust pressure and temperature conditions. J. Geophys. Res. Solid Earth 117 (B3), 213–235.
Vrolijk, P.J., Urai, J.L., Kettermann, M., 2016. Clay smear: review of mechanisms and applications. J. Struct. Geol. 86, 95–152.
Wang, L.S., Li, C., Liu, S.W., Li, H., Xu, M.J., Wang, Q., Ge, R., 2003. Geotemperature gradient distribution of Kuqa foreland basin, North of Tarim, China. Chin. J. Geophys. 46 (3), 403–407.
Welsh, M.J., Knipe, R.J., Souque, C., Davies, R.K., 2009. A Quadshear kinematic model for folding and clay smear development in fault zones. Tectonophysics 471, 185–202.
Wong, T.F., David, C., Zhu, W.L., 1997. The transition from brittle faulting to cataclastic flow in porous sandstones: mechanical deformation. J. Geophys. Res. 102 (B2), 3009–3025.
Wong, T.F., David, C., Menéndez, B., 2004. Mechanical compaction. In: Guéguen, Y., Boutéca, M. (Eds.), Mechanics of Fliud-saturated Rocks. Elsevier Academic Press, Amsterdam, pp. 55–114.
Wong, T.F., Baud, P., 2012. The brittle-ductile transition in porous rock: a review. J. Struct. Geol. 44, 25–53.
Yang, M.H., 2013. Study on Acoustic emission evolution characteristic of Plastic and brittle Coal failure process. Adv. Mater. Res. 2398–2403.
Yielding, G., Freeman, B., Needham, T., 1997. Quantitative fault seal prediction. AAPG Bull. 81 (6), 897–917.
Zhuo, Q.G., Li, Y., Song, Y., Zhang, X.Z., Zhao, M.J., Fang, S.H., Liu, S.B., Lu, X.S., 2013. Evolution of Paleogene saline deposits and effectiveness of traps in Kelasu tectonic zone, Kuqa depression, Tarim basin. Pet. Geol. Exp. 35 (1), 42–47.